Tunnel Diode Oscillator in an Open Structure

EIKICHI YAMASHITA, MEMBER, IEEE, AND JACK R. BAIRD, MEMBER, IEEE

Abstract—**This paper describes a theoretical and experimental evaluation of the oscillation conditions of a microwave tunnel diode integrally mounted at the feed point of a semicircular loop antenna. The oscillation conditions are based on a quasi-linear equivalent circuit where the diode load impedance is the complex radiation impedance of the semicircular loop antenna. The results of a radiation impedance calculation based on a Fourier transform method are presented. Diode fabrication techniques are described and experimental results are reported to be consistent with the theory.**

Introduction

THE OSCILLATION characteristics of a microwave tunnel diode mounted in a rectangular waveguide were analyzed in a previous paper [1]. There it was shown that for simple configurations it is possible to calculate the oscillation frequency as a function of the dimensions of the microwave structure.

This method is extended here to the analysis of a tunnel diode integrally constructed at the "feed point" of a small semicircular loop antenna. It has been demonstrated that detector diodes [2] fabricated in this configuration can be used in the low-loss reflecting beam waveguide [3] and in rectangular waveguide. A similar diode structure in a rectangular waveguide has recently been used as an avalanche diode oscillator [4] with operating frequencies as high as 140 GHz.

The oscillation conditions for a given tunnel diode oscillator are determined by the load impedance connected to the diode. In this loop configuration, the load impedance is simply the complex radiation impedance of the semicircular whisker wire acting as an antenna. This paper presents the results of a calculation of this radiation impedance as a function of frequency. Oscillation characteristics are analyzed based on this load impedance, and experimental results are described.

Theoretical Considerations

Tunnel diode oscillators are approximately analyzed on the basis of their ac equivalent circuit assuming a quasi-linear negative resistance. The series equivalent impedance of a tunnel diode [1] is given by

$$Z_0 = R_0 + jX_0 \tag{1}$$

$$R_0 = R_s - \frac{R_-}{1 + \omega^2 C^2 R_-^2} \tag{2}$$

$$X_0 = -\frac{\omega C R_-^2}{1 + \omega^2 C^2 R_-^2} \tag{3}$$

where ω is the angular frequency, R_- is the negative resistance, C is the junction capacitance, and R_s is the spreading resistance. This definition of the diode impedance does not include effects of the diode package or lead wire, but describes only the junction and the bulk semiconductor.

Given a general load impedance

$$Z_L = R_L + jX_L \tag{4}$$

the following conditions [1] are deduced for steady state:

$$R_L + R_0 = 0 \tag{5}$$

and

$$X_L + X_0 = 0. \tag{6}$$

Though these two conditions must be satisfied at the same time, they do not impose a severe restriction on the oscillator, because the diode resistance R_0 is a function of both the bias voltage and the oscillation amplitude.

For a tunnel diode mounted in some type of microwave structure, the load impedance is the radiation impedance at the two terminals of the semiconductor chip. The calculation of the radiation impedance of this semicircular loop antenna [5] is quite involved and will not be derived in this paper. Except in detail, the method of calculation is similar to the principle proposed by Rhodes [6] to formulate the radiation impedance of a planar antenna in the transformed plane.

The calculation proceeds as follows.

1) From Maxwell's equations, a wave equation is obtained which relates the vector potential to the current density distribution.
2) A polar coordinate system is introduced to fit the configuration of the loop.
3) The Fourier transform is applied to the z coordinate of all field quantities.
4) A Fourier series expansion is applied to the θ coordinate of all field quantities.
5) Solutions to the ρ coordinate equation are obtained as Bessel and Hankel functions, assuming that the diameter of the wire is much smaller than the radius of a loop.
6) A variational expression for the radiation impedance (or load impedance Z_L) in the configuration space

$$Z_L = -\frac{1}{I^2}\int E(r)\cdot J(r)^* dV \tag{7}$$

is converted to the transformed space by the use of Parseval's theorem.

Manuscript received September 16, 1966; revised March 20, 1967. The work reported in this paper was supported by RADC Contract AF 30(602)-3830. This paper is based on part of a dissertation submitted by E. Yamashita in partial fulfillment of the requirement for the Ph.D. degree at the University of Illinois, and was prepared partly by the support of Army Research Grant DA G-646.

The authors are with the Dept. of Elec. Engrg., University of Illinois, Urbana, Ill.

$$Z_L = -\frac{1}{2\pi I^2}\int\int\int \tilde{E}(\rho, \theta, \beta)\cdot\tilde{J}(\rho, \theta, \beta)^*\rho d\rho d\theta d\beta \quad (8)$$

where β is the variable in the transformed coordinate, I is the magnitude of the driving point current, and $\tilde{E}$ and $\tilde{J}$ are the Fourier-transformed quantities.

The trial function for the current density distribution assumes a sinusoidal variation along the loop wire with no variation in the cross section of the wire. The insulation layer of the coaxial structure is so thin that its effect on the preceding current distribution is neglected.

The results of this impedance calculation are

$$R_L = \frac{\eta_0(k_0a)^3a\tan^2(k_0a\pi)}{4\pi}\sum_{m=0}^{\infty}\cdot\frac{\epsilon_{0m}}{(k_0^2a^2-m^2)^2}\int_0^{k_0}\frac{\chi}{(k_0^2-\chi^2)^{1/2}}\cdot\left[\frac{2\sin\left(\frac{\beta d}{2}\right)}{\beta d}\right]^2\left[\frac{4J_1\left(\frac{\chi d}{2}\right)}{\chi d}\right]^2\cdot[J_{m-1}^2(\chi a)+J_{m+1}^2(\chi a)]d\chi \quad (9)$$

$$X_L = -\frac{\eta_0(k_0a)^3a\tan^2(k_0a\pi)}{4\pi}\sum_{m=0}^{\infty}\frac{\epsilon_{0m}}{(k_0^2a^2-m^2)^2}\cdot\int_0^{k_0}\frac{\chi}{(k_0^2-\chi^2)^{1/2}}\cdot\left[\frac{2\sin\left(\frac{\beta d}{2}\right)}{\beta d}\right]^2\left[\frac{4J_1\left(\frac{\chi d}{2}\right)}{\chi d}\right]^2\cdot[J_{m-1}(\chi a)N_{m-1}(\chi a)+J_{m+1}(\chi a)N_{m+1}(\chi a)]d\chi + \frac{\eta_0(k_0a)^3a\tan^2(k_0a\pi)}{2\pi^2}\sum_{m=0}^{\infty}\frac{\epsilon_{0m}}{(k_0^2a^2-m^2)^2}\cdot\int_0^{\infty}\frac{\Lambda}{(k_0^2+\Lambda^2)^{1/2}}\cdot\left[\frac{2\sin\left(\frac{\beta d}{2}\right)}{\beta d}\right]^2\left[\frac{4J_1\left(\frac{\Lambda d}{2}\right)}{\Lambda d}\right]^2\cdot[I_{m-1}(\Lambda a)K_{m-1}(\Lambda a)+I_{m+1}(\Lambda a)K_{m+1}(\Lambda a)]d\Lambda \quad (10)$$

where

$\eta_0 = 120\pi$ (ohms)
$k_0 = 2\pi/\lambda$
a = the radius of the loop
d = the diameter of the wire
$\beta^2 = k_0^2-\chi^2 = k_0^2+\Lambda^2$
$\epsilon_{0m} = \begin{cases} 1 & (m=0) \\ 2 & (m>0) \end{cases}$
$J_m(\chi a)$ and $N_m(\chi a)$ are Bessel functions
$I_m(\Lambda a)$ and $K_m(\Lambda a)$ are modified Bessel functions.

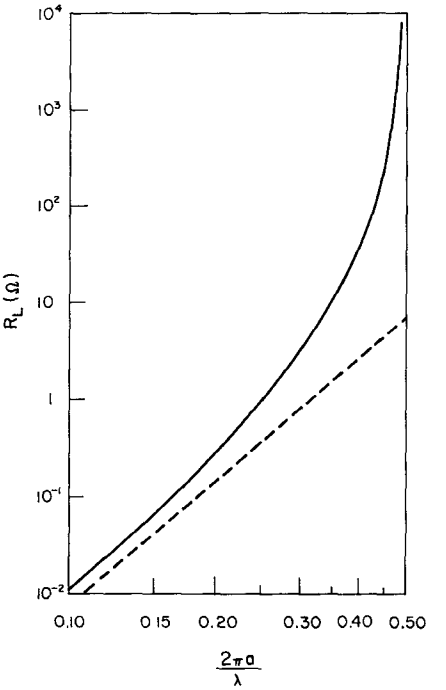

Fig. 1. The radiation resistance R_L of a semicircular loop whisker versus the loop radius a and the wavelength λ. The solid line shows values by (9), the dotted line the classical formula (11).

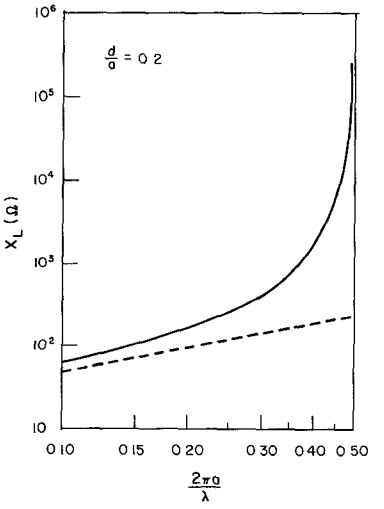

Fig. 2. The reactance X_L of a semicircular loop whisker versus the loop radius a and the wavelength λ, for $d/a=0.2$. The solid line shows the values by (10), the dotted line the classical formula (12).

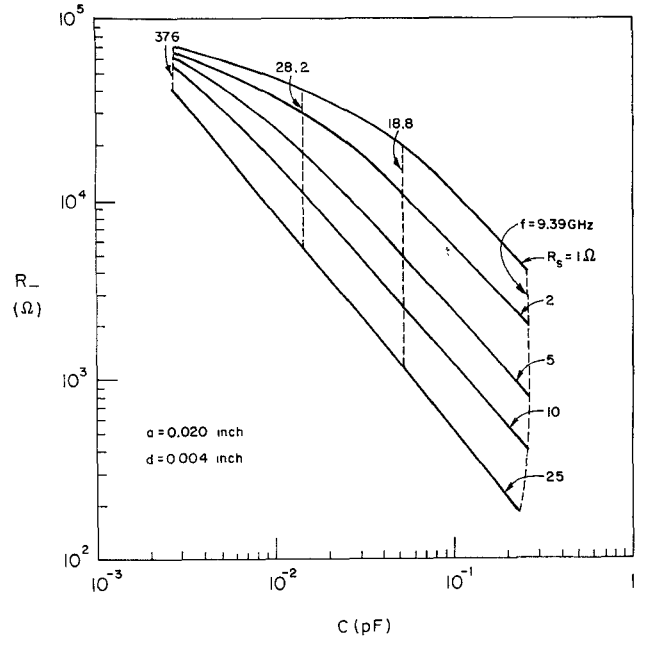

Fig. 3. The graph showing possible combinations of the negative resistance R_-, the junction capacitance C, oscillation frequency f, and spreading resistance R_s for a given loop radius a and whisker wire diameter d.

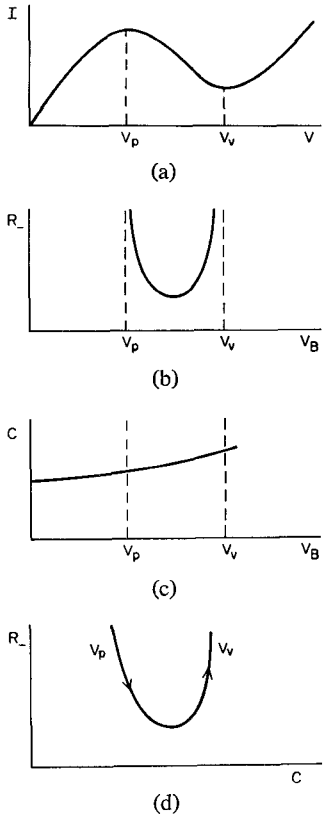

Fig. 4. Characteristics of the junction impedance. (a) Static V–I characteristics of a tunnel diode. (b) The differential negative resistance R_- versus the bias voltage V_B. (c) The junction capacitance C versus the bias voltage V_B. (d) A locus of C and R_- for the change of the bias voltage.

The low-frequency limit ($k_0a \to 0$) of (9) reduces to the classical radiation resistance of a semicircular loop antenna [7].

$$R_L = 10\pi^2(k_0a)^4 \tag{11}$$

For very low frequencies, the reactance given by (10) is very close to the reactance of a semicircular loop as calculated from a static field approximation [8]

$$X_L = \omega L = \frac{\omega\mu_0 a}{2}\left[\ln\left(\frac{16a}{d}\right) - \frac{7}{4}\right]. \tag{12}$$

The solid curves of Figs. 1 and 2 show the real and imaginary part of the load impedance as a function of frequency. These curves were obtained by numerical techniques applied to (9) and (10). The dashed lines indicate values obtained from (11) and (12).

Having calculated the radiation impedance of a semicircular loop antenna, the problem now remains to determine the frequency of oscillation and the power output from a tunnel diode with this load impedance. The oscillation conditions are too complicated to express the oscillation frequency explicitly.

A graphical technique has been developed to indicate necessary combinations of C, R_-, f, and R_s for a given loop radius and wire diameter. Figure 3 shows an example of this technique. It can be seen that the oscillation frequency is almost entirely dependent upon the junction capacitance. A smaller loop radius, of course, would yield a smaller load inductance and a higher frequency. Figure 4(b) and 4(c) indicates qualitatively the variation of C and R_- with the diode bias voltage. These two curves can be combined as Fig. 4(d) and the intersection of this curve with Fig. 3 would predict the variation of oscillation frequency with bias voltage. The capacitance scale of Fig. 4(d) is considerably more expanded than the corresponding scale of Fig. 3.

Experimental Investigation

With this oscillator structure, one has to develop a method of fabricating a tunnel diode with a semicircular loop and also a method of measuring the oscillation characteristics. The p–n junction of a tunnel diode requires a thin junction layer between highly doped p- and n-type semiconductors. An alloyed junction tunnel diode fabricated from a point-contact configuration [9] is convenient for microwave experiments. However, the zinc whisker normally used is mechanically too soft for the loop wire. Therefore, a zinc-plated tungsten wire was employed as a whisker in this investigation.

A small sample of a GaAs crystal with a selenium donor concentration about 10^{19} cm^{-3} was nickel-plated and then soldered to one end of a 0.75 inch long, 0.030 inch diameter tungsten rod. The end of the tungsten rod had previously been ground to a diameter of 0.020 inch and nickel-plated. Copper was electroformed onto the crystal and the end of

the tungsten rod, and the rod was machined to a uniform diameter of 0.030 inch. A dielectric layer was obtained by dip-coating about half of the length of the rod in glyptal. A thin layer of silver paint provided the electrical contact for electroplating an outer conductor of copper. The copper was then machined to a uniform diameter of 0.087 inch and a portion of the copper was machined away to expose the dielectric layer. The end of the rod was then lapped on a surface plate until the crystal surface was exposed. The entire semiconductor was then polished and etched with a solution [9] of NaOH and H_2O_2.

A short tungsten wire of 0.004 inch diameter was bent into a U shape and annealed in an oven to obtain mechanical stability. This wire was spot-welded to the inside surface of a metal (CuNi) tube. The wire was etched electrochemically in a moderate solution of NaOH to make a very sharp point and therefore to make a very small junction area. Soon after etching, the sharp point was plated with zinc in a solution of ZnCN, NaOH, and β-napthol.

The semiconductor section was pressed into the tube and the whisker was guided into a slot which had been made on the copper rod. After making light contact between the GaAs crystal surface and the whisker point, a forming current was applied to the contact from a capacitor (0.01 μF) through a resistor [10] (50 ohms). The capacitor was previously charged to 3 to 5 volts. The cross-sectional view of the fabricated tunnel diode is shown in Fig. 5.

The fabricated tunnel diode was mounted through a hole in a conducting ground plane as shown in Fig. 6(a). A 60 Hz voltage was used to sweep the bias voltage across the negative resistance region, and the same bias voltage was used as the horizontal sweep on an oscilloscope. The bias current I_B through the tunnel diode and the microwave power were displayed on the oscilloscope to measure R_-, I_B, f, and P_r, for each value of bias voltage. R_- and I_B were evaluated from a photo of the 60 Hz V–I characteristics taken from the oscilloscope. f and P_r were measured with the video detector which had been calibrated against a bolometer. Figure 6(b) shows the block diagram of the measurement system.

Figure 7 shows the measured points of R_- and f for several tunnel diodes plotted upon the curves of Fig. 3. The spread of values is due to the deviation of the pressure in the p–n junction, the whisker point area, the forming current, the crystal surface state, and/or the ohmic contact resistance.

The spreading resistance may be the largest part of R_s, though other ohmic losses are included in R_s implicitly. The thickness of the zinc layer on the surface of the whisker was estimated to be as thin as one micron, but it was thick enough to produce the tunneling effect. The minimum capacitance obtained in these experiments was approximately 0.06 pF. Young et al. [10] reported a junction capacitance of about 0.04 pF for tunnel diodes made by this alloyed junction of n-GaAs and zinc. The static characteristics varied from diode to diode as shown in Table I. However, the measured ratios of the peak current I_p, over

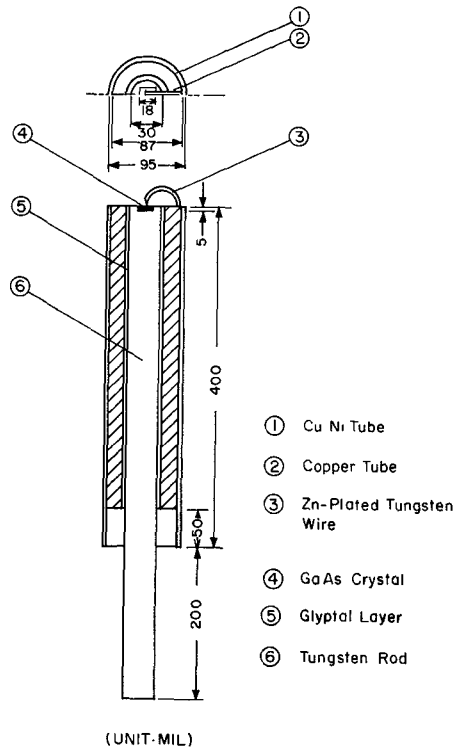

Fig. 5. Sketch of the fabricated tunnel diode.

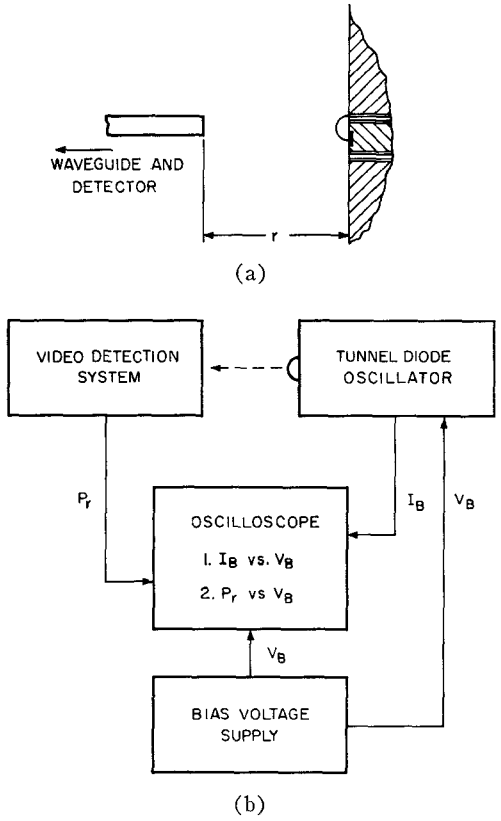

Fig. 6. The measurement method of oscillation characteristics. (a) The measurement of the radiation power P_r and the oscillation frequency f versus the distance r and the bias voltage V_B. (b) The block diagram of this measurement.

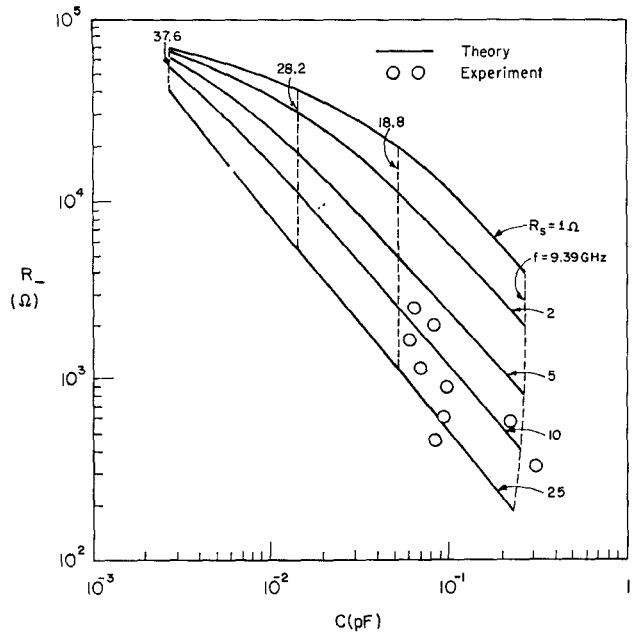

Fig. 7. The negative resistance R_- and the oscillation frequency f were measured and plotted as small circles on the graph of Fig. 3.

TABLE I

MEASURED dc CHARACTERISTICS OF SOME TUNNEL DIODES

No.	I_p(mA)	I_v(mA)	V_p(mV)	V_v(mV)	I_p/I_v
2	0.64	0.23	230	570	2.8
6	0.48	0.29	220	480	1.7
8	1.5	0.51	320	650	2.9
9	1.6	0.36	280	750	3.8

the valley current I_v, are similar to the values reported in the literature [10].

The basic assumption in this method of analysis is that there is a certain range of quasi-linear negative resistance which allows oscillations. Suppose that V_1 and V_2 are the ends of the quasi-linear negative resistance region. The oscillation voltage grows from V_B until it is limited by V_1 or V_2. Therefore, the oscillation power from the negative resistance is given by the smallest value of

$$P = \frac{|V_B - V_1|^2}{2R_-} \quad \text{or} \quad \frac{|V_B - V_2|^2}{2R_-}. \tag{13}$$

This relation is normalized and plotted as a solid line in Fig. 8(b). The experimentally observed power output for three different diodes was normalized and plotted with the above curve.

Part of this power is dissipated in the semiconductor bulk [11], so that the power delivered to the load radiation resistance is given by

$$P_L = \left(\frac{R_L}{R_L + R_s}\right) P. \tag{14}$$

This expression obviously gives approximate values because of the diode nonlinearity.

Since the actual loop radius of this particular diode was about 0.025 inch, the radiation resistance should be corrected to 0.45 ohm. This correction does not affect R_-, C, or R_s, because R_s is much larger than R_L in this case. The experimental data show that: $R_s = 8.4$ ohms, $|V_B - V_1| = 0.16$ volt, and $R_- = 1500$ ohms. Therefore, (14) gives $P_L = 0.19$ μW.

Experimentally, only part of the power was received with a waveguide aperture at a distance r from the center of the loop. When A_e is the effective area of the receiving waveguide antenna and P_i is the radiation power intensity at r, the received power P_r is given by

$$P_r = A_e P_i. \tag{15}$$

Figure 9 shows the observed values of P_r as a function of r for the above diode. Since the standing wave effect between the loop and the waveguide system is negligible at $r = 50$ mm as seen in Fig. 9, the extrapolated value of P_r at this point, 7.5×10^{-3} μW, can be compared with the theoretical estimation. The wavelength λ was 17.8 mm. Since estimated values are $P_L \cong 0.19$ μW, $A_e \cong 5.4 \times 10^2$ mm^2, and $P_i \cong 4 \times 10^{-2}$ μW/mm^2, in this case, (15) gives $P_r \cong 2 \times 10^{-3}$ μW. This is in the same order of the experimentally measured value 7.5×10^{-3} μW at $r = 50$ mm.

The angular distribution of the radiation power intensity was observed for diode No. 4. Since the oscillation frequency is relatively low in this case, the current distribution is almost constant along the loop. Consequently, the angular dependence of the detected power is expected to be almost constant. Measured values indicated in Table II confirm this experimentally.

The bias voltage dependence of oscillation frequency is due to a change in the barrier capacitance with bias voltage. A low-frequency experiment [12] shows that the capacitance is increased about 6 percent per 100 mV in the negative resistance region for a germanium tunnel diode. In the laboratory, a tunnel diode with a loop whisker oscillated over the frequency range from 20.85 to 20.48 GHz when the bias voltage was changed from 240 to 320 mV. According to the theoretical curves shown in Fig. 3, this change of oscillation frequency corresponds to an increase of the barrier capacitance of 6.3 percent per 100 mV. Although a GaAs crystal was used in this case, the experimentally obtained value is explained well by the theory.

A second harmonic component of the oscillation was also observed for some tunnel diodes, though the detected power was at an extremely low level. Data of the second harmonic showed $f = 31.2$ GHz, $P_r = 0.028$ μW, and $r = 7.8$ mm, for the tunnel diode No. 8; and $f = 32.8$ GHz, $P_r = 0.012$ μW, and $r = 10$ mm, for the tunnel diode No. 9.

The radiation resistance at 32 GHz is about 14 ohms for $a = 0.020$ inch. Therefore, a high percentage of the second harmonic power would be radiated while a large part of

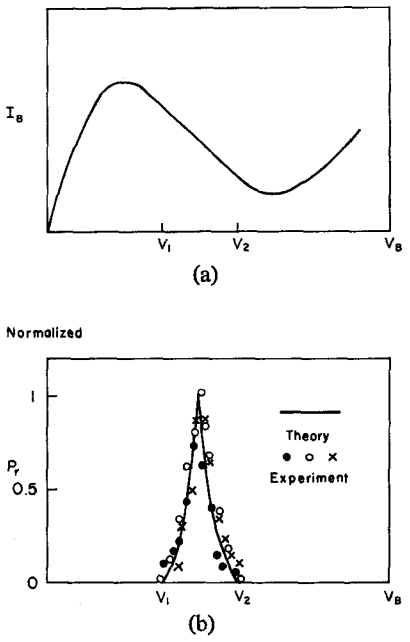

Fig. 8. The bias voltage dependence of oscillation power P_r. (a) A quasi-linear negative resistance region limited by V_1 and V_2. (b) The estimated and measured bias dependence.

TABLE II

ANGULAR DEPENDENCE OF RADIATION POWER OF A TUNNEL DIODE

θ (Radian)	Normalized P_r
$\frac{1}{8}\pi$	9×10^{-1}
$\frac{1}{4}\pi$	1
$\frac{1}{2}\pi$	1
$\frac{3}{4}\pi$	1
$\frac{7}{8}\pi$	9×10^{-1}

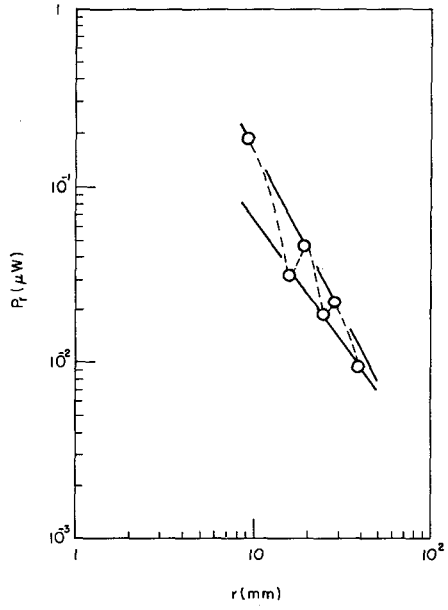

Fig. 9. The radiated power P_r versus the distance r.

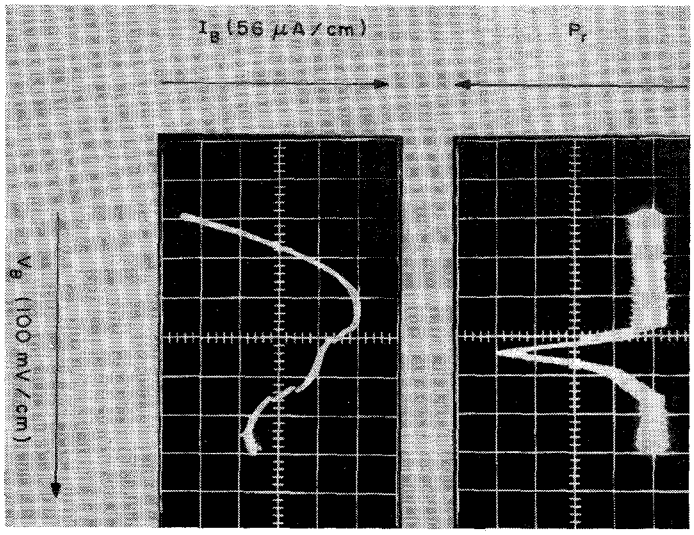

Fig. 10. A typical oscilloscope figure seen in the measurement system of Fig. 6.

the fundamental power would be dissipated in R_s. This might be the reason why the second harmonic power was nearly equal to the fundamental power. Figure 10 shows a typical curve obtained on the oscilloscope. The upper curve is the bias voltage dependence of the received power by a waveguide aperture at the distance r, and it gives the oscillation frequency and oscillation voltage amplitude experimentally. The lower curve is the bias voltage dependence of the bias current, and it is used for the negative resistance measurement.

CONCLUSION

The oscillation characteristics of a tunnel diode with a semicircular loop whisker are theoretically estimated by the radiation impedance method. Experimental observation shows good agreement with this theory. However, both experiment and theory indicate that the radiation impedance of this structure is not the most suitable for obtaining the highest frequency oscillation. The inductive reactance of the semicircular loop is too large which causes the oscillation frequency to be well below the frequency obtained in other mounting configurations. The load resistance at the oscillating frequency is too low to efficiently couple power from the tunnel diode. The radiation resistance could be enhanced by changing the shape of the loop or placing it in some resonant structure.

The tunnel diode made of n-GaAs and zinc also has the disadvantage of gradual degradation of performance in time. This problem has recently been mentioned in Burrus [13], and it is believed to be a result of zinc diffusion into n-type side of the junction.

It is believed that this method of calculating the load impedance can be used in other microwave negative resistance devices such as the Gunn effect or avalanche diode to estimate the effect of microwave structure on oscillation or amplification.

ACKNOWLEDGMENT

The authors would like to express appreciation to Prof. P. D. Coleman, the director of this project, for his assistance and advice, to Dr. C. A. Burrus, Bell Telephone Laboratories, Inc., for his cooperation in connection with the fabrication process of tunnel diodes, and to Dr. S. T. Smith, Naval Research Laboratory, for his helpful comments on this manuscript.

REFERENCES

[1] E. Yamashita and J. R. Baird, "Theory of a tunnel diode oscil-, lator in a microwave structure," *Proc. IEEE*, vol. 54, pp. 606–611 April 1966.
[2] J. E. Degenford, J. R. Baird, and E. Yamashita, "A magnetic loop, diode detector compatible with microwave and beam waveguide," *IEEE Trans. Microwave Theory and Techniques (Correspondence)*, vol. MTT-13, pp. 380–382, May 1965.
[3] J. E. Degenford, M. D. Sirkis, and W. H. Steier, "The reflecting beam waveguide," *IEEE Trans. Microwave Theory and Techniques*, vol. MTT-12, pp. 445–453, July 1964.
[4] L. S. Bowman and H. J. Muller, "Oscillation of silicon *p-n* junction avalanche diode in the 50 to 140 GHz range," *Proc. IEEE (Letters)*, vol. 54, pp. 1080–1081, August 1966.
[5] Final Rept., RADC Contract AF 30(602)-3830.
[6] D. R. Rhodes, "On a fundamental principle in the theory of planar antennas," *Proc. IEEE*, vol. 52, pp. 1013–1021, September 1964.
[7] J. D. Kraus, *Antennas*. New York: McGraw-Hill, 1950.
[8] W. R. Smythe, *Static and Dynamic Electricity*. New York: McGraw-Hill, 1950.
[9] C. A. Burrus, "Gallium arsenide Esaki diodes for high-frequency applications," *J. Appl. Phys.*, vol. 32, pp. 1031–1036, June 1961.
[10] D. T. Young, C. A. Burrus, and R. C. Shaw, "High efficiency millimeter-wave tunnel diode oscillators," *Proc. IEEE (Correspondence)*, vol. 52, pp. 1260–1261, October 1964.
[11] H. J. Oguey, "Analysis of the frequency and power performances of tunnel diode generators," *IEEE Trans. Microwave Theory and Techniques*, vol. MTT-11, pp. 412–419, September 1963.
[12] L. Esaki and J. Miyahara, "A new device using the tunneling process in narrow *p-n* junctions," *Solid-State Electronics*, vol. 1, no. 1, pp. 13–21, 1960.
[13] C. A. Burrus, "Millimeter-wave point-contact and junction diodes," *Proc. IEEE*, vol. 54, pp. 575–587, April 1966.

Solid-State YIG Serrodyne

DENIS C. WEBB, MEMBER, IEEE, AND ROBERT A. MOORE, MEMBER, IEEE

Abstract—**Theory and operation of a serrodyne based upon phase velocity modulation of magnetostatic modes in YIG are described. Sources of limitation on the spectral performance are evaluated in terms of measured device parameters. The most critical sources of unwanted spectral generation are flyback time, nonlinear current sawtooth, logarithmic phase variation, and variation in attenuation with applied magnetic bias. Design and operation of a *C*-band stripline device is described. All unwanted sidebands were suppressed by 22 dB over the desired signal output, limited primarily by the flyback time.**

INTRODUCTION

A MICROWAVE signal can be converted to a single sideband by sawtooth modulation of its phase velocity in a transmission or delay medium. Such a process is known as serrodyne frequency translation. It has proved useful in a wide variety of microwave applications [1] including Doppler simulation and correction, scanning of antenna arrays, and frequency shifting in microwave relay systems. The particular delay device that has received the greatest serrodyne application is the traveling wave tube. In the TWT serrodyne, the modulation is applied to the helix or cathode, causing a periodic bunching of the electron beam. Cumming [2] analyzed and tested this device in detail, developing and evaluating a set of performance criteria. With slight modification, these criteria can be applied to any phase modulable device such as the klystron, ferrite phase shifter [3] or crystal modulator [4], all of which have been used as serrodynes.

In this paper a *C*-band solid-state serrodyne is described. The frequency offset is obtained by using the magnetically variable phase velocity of magnetostatic modes propagating in a yttrium iron garnet rod. In the following sections, a brief outline of phase properties of magnetostatic modes in rods is first given, followed by design and performance characteristics of the YIG serrodyne. Spectral purity is discussed based on criteria developed by Cumming. Insertion loss and modulation power are also discussed. Minimal size, weight, and modulation power make the present device especially attractive for satellite application.

Manuscript received September 12, 1966; revised February 17, 1967.

D. C. Webb is with W. W. Hansen Laboratories of Physics, Stanford, Calif. 94305. He was formerly with the Microwave Physics Group, Aerospace Division, Westinghouse Defense and Space Center, Baltimore, Md. 21203

R. A. Moore is with the Microwave Physics Group, Aerospace Division, Westinghouse Defense and Space Center, Baltimore, Md. 21203

PHASE PROPERTIES OF YIG RODS

It was noted above that the traveling wave tube relies upon modulation of the electron velocity to achieve frequency translation. As Cumming pointed out, when beam modulation is employed, the wave velocity is established at the time the waves enter the device. By contrast, in the mag-